Effect of secondary substituent on the physical properties, crystal structures, and nanoparticle morphologies of (porphyrin)Sn(OH)$_2$: diversity enabled *via* synthetic manipulations†

Suk Joong Lee, Rebecca A. Jensen, Christos D. Malliakas, Mercouri G. Kanatzidis, Joseph T. Hupp* and SonBinh T. Nguyen*

A highly efficient porphyrin synthesis facilitates a systematic investigation of the effects that secondary substituents have on the physical properties, crystal structures, and nanoparticle morphologies of amphiphilic (porphyrin)Sn(OH)$_2$.

The enormous potential that metalloporphyrins possess in catalysis, photochemistry, sensing, and as optical devices has made them favorite building blocks in the emerging field of molecular materials.[1] With attractive structural features such as large bulk, rigid planarity, and a highly conjugated framework that can be readily modified with a variety of functional groups, porphyrins can be assembled into supra- and super-structures in a relatively facile manner.[2] Indeed, porphyrin building blocks have been used extensively in the construction of nano-, micro-, and macroscopic structures,[3] including nanomaterials[4] using π–π interactions, electrostatic interactions, and metal coordination with appropriate choice of primary substituents. Largely overlooked has been the manipulation of secondary substituents (*i.e.*, substituents that are not directly bonded to the porphyrin ring) to engender van der Waals interactions beyond the immediate porphyrin ring. Herein, we demonstrate the potential for using such substituents to influence the physical properties, crystal structures, and nanocrystal morphologies of materials based on amphiphilic (porphyrin)Sn(OH)$_2$. This endeavor was facilitated by applying the Lindsey dipyrromethane methodology[5] to quickly generate secondary substituent diversity on a porphyrin framework.

The barriers most often encountered in systematic investigations of porphyrin-based materials are synthetic in nature. Such studies, especially those concerning crystalline phases, often require macroscopic quantities of materials; yet porphyrins are typically obtained only in low yield and large crystals of porphyrins are difficult to grow. The latter challenge can be addressed by growing porphyrin nanocrystals[4] and assembling them into macroscopic objects. In this spirit, we have recently demonstrated the facile hierarchical assembly of crystalline porphyrin nanorods into micron-size prisms.[4a] Under highly agitated conditions, [5,15-bis(pyridyl)-10,20-diarylporphyrin]Sn(OH)$_2$, possessing both hydrogen-bond-acceptor and -donor functionalities, proved to be an ideal precursor for growing amphiphilic nanocrystals that could subsequently be assembled, with the assistance of surfactants, into macroscopic objects. In this communication, we focus on a strategy for quickly generating porphyrin nanocrystals displaying diverse morphologies from easily accessible (porphyrin)Sn(OH)$_2$ molecular precursors. Our premise is that simple changes in the van der Waals surfaces of the (porphyrin)Sn(OH)$_2$ building blocks, tuned *via* secondary substituents, can significantly affect the morphologies of the crystals and nanocrystals grown from these molecules.[4a]

The condensation reaction between 4-pyridylaldehyde and the corresponding *meso*-aryldipyrrolemethane affords 5,15-bis(pyridyl)-10,20-diarylporphyrin in excellent yield (26–35%) (Scheme 1). Subsequent metallation with SnCl$_2$ and hydrolysis with K$_2$CO$_3$ readily affords the dihydroxytin derivatives **1–3**. In contrast to traditional multistep methods for dipyridyl porphyrin synthesis where the dipyridyl moieties are elaborated through cross-coupling reactions,[6] the overall yield of the sequence shown in Scheme 1 is high (19–30%) by porphyrin standards, making large quantities of **1–3** readily available in two steps. As the *meso*-aryldipyrrolemethane can be accessed readily in one step from the corresponding aldehyde and pyrrole,[5] a wide range of secondary aryl substituents can be deployed to facilitate subsequent investigations into nanocrystal growth.

Using the Shelnutt strategy,[4c] we have recently prepared several porphyrin nanorods and plates from (porphyrin)Sn(OH)$_2$ with different main-ring hydrophobicity and pyridine–pyridine distances.[4a] Following this protocol, when an ethanolic solution of **1** or **2** is injected into stirring water at room temperature (rt), a light brown suspension is obtained. Analysis by scanning electron microscopy (SEM) reveals these porphyrin suspensions to be collections of fairly uniform diamond plates that are 400–600 nm long for **1** and 750–900 nm long truncated bipyramidal particles for **2** (Fig. 1a and 1c, respectively). However, for the more hydrophobic (porphyrin)Sn(OH)$_2$ **3**, only an amorphous solid is observed (Fig. 1e).

Interestingly, when a solution of **1** in ethanol is injected in water and agitated *via* microwaves at 45 °C for 1 min, hexagonal plates ~2 μm long are obtained. For **2**, well-defined ~2 μm long herring bone double blades result. Both materials are remarkably homogeneous in

Northwestern University, Department of Chemistry, 2145 Sheridan Road, Evanston, IL 60208, USA. E-mail: j-hupp@northwestern.edu; stn@northwestern.edu; Fax: +847-491-7713; Tel: +847-467-3347

Scheme 1
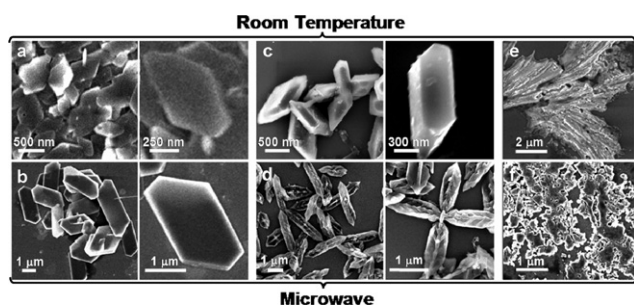
Fig. 1 SEM images of the different nanocrystal morphologies obtained from porphyrin building blocks **1–3** under various conditions; a) and b) from **1**, c) and d) from **2**, e) and f) from **3**. Conditions: a), c), and e): rt, stirring; b), d), and f): 45 °C, microwaves.

size (Fig. 1b and 1d). Again, **3** gives only undefined aggregates (Fig. 1f) under these conditions.

The two nanocrystal samples from **1** exhibit powder X-ray diffraction (PXRD) patterns (Fig. 2) that closely resemble the diffraction pattern for a single crystal sample grown under non-agitated conditions. Such similarities imply that the corresponding unit cells for the three samples are identical. The PXRD patterns for nanocrystals and single crystals obtained from **2** are likewise similar (ESI†‡), suggesting a conservation of the molecular packing arrangement.

For amphiphilic (porphyrin)Sn(OH)$_2$, the pyridyl substituents and Sn(OH)$_2$ core of one porphyrin can hydrogen-bond to adjacent molecules in the solid state to afford ordered porphyrin arrays.[4c,7] Because direct coordination of the pyridyl nitrogen to the hexacoordinate Sn(IV) center is not expected,[7] variously weighted combinations of hydrogen bonding, hydrophobic interactions, and π–π stacking can account for the formation of well-ordered arrays of (porphyrin)Sn(OH)$_2$—with the different weightings from secondary substituents resulting in different nanocrystals (Fig. 3).

Interestingly, the single crystal structure of **1** indicates that **1** uses only one of its two pyridine/OH pairs for hydrogen bonding. The result is the relatively symmetrical head-to-tail arrangement shown in Fig. 3 (right column). The comparatively small size of the methoxy
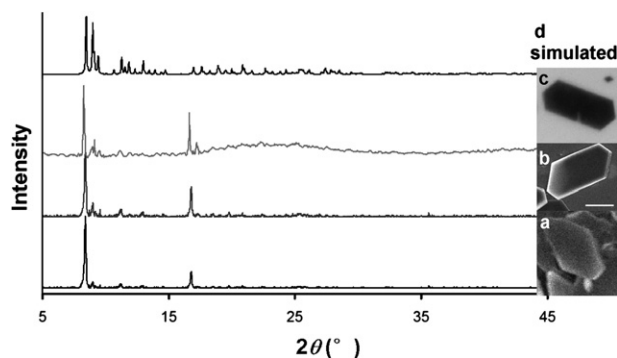
secondary substituents in **1** uniquely enables one pendant pyridyl group to approach closely enough to the axial OH ligand of an adjacent porphyrin to achieve direct interaction. In contrast, **2**, which features slightly larger dibutoxy secondary substituents, packs with longer distances between its pyridyl groups and the OH ligands of the adjacent porphyrin cores. This packing arrangement necessitates mediation by water to form a network of Sn–OH–H$_2$O–N hydrogen-bonding bridges (Fig. 3, third column) that are less dense than that in **1**, with two crystallographically independent porphyrin molecules alternating in a pseudo-herringbone fashion. One of the two porphyrins enlists both of its OH groups for H-bonding while the other only employs its pyridyl groups, thereby allowing a water molecule to be accommodated between the two porphyrins.

The (2,6-dialkoxy)phenyl substituents in **1** and **2** pack so as to render two faces of the crystals hydrophobic while the orthogonal HO–Sn–OH moiety makes the remaining face more hydrophilic (Fig. 3, looking down the diagonal direction of the *abc*-axes), suggesting a natural tendency for crystal growth in water to occur faster along the hydrophilic direction than the hydrophobic one, resulting in nanocrystals that are flat and long. In **2**, where water molecules must be recruited as structural components and the secondary substituents on the phenyl ring are more hydrophobic, crystal growth along the hydrophilic direction presumably becomes more retarded relative to that in **1**, resulting in thicker nanoplates.

In the case of **3**, the bulky and more hydrophobic dioctoxyphenyl groups force the porphyrins apart and prevent intermolecular H-bonding (Fig. 3, third column). These differences are manifested most clearly in the contact angle experiments shown in the fourth column of Fig. 3 where thin films[8] of porphyrins **1–3** repel water at different contact angles. Together with the structural data presented above, these results illustrate how seemingly small changes to porphyrin building blocks can lead to significant changes, not only in the physical properties of the thin films derived from them, but also in the growth and morphology of the corresponding nanocrystalline materials.

As multi-porphyrin materials, the crystalline nanoparticles obtained from **1** and **2** exhibit absorption and emission spectra that differ considerably from those of the monomers (ESI,†Fig. S1 and S2).[4c,9] For example, compared to monomer **2** in ethanol, which show a B-band at 425 nm and Q-bands at 557 and 593 nm, the extinction spectrum of the nanoparticle colloidal dispersions in water are more complicated. The B-band is split, with sub-peaks at 426, 428 and 452 nm, while the Q-bands red-shift slightly to 567 and 603 nm. The emission spectrum of nanoparticles of **2** shows multiple bands at 611, 633, 661, and 693 nm, while only two bands at 604 and 659 nm are seen for a solution of **2**.

In summary, crystalline nanoparticles of [5,15-bis(pyridyl)-10,20-diarylporphyrin]Sn(OH)$_2$ with a variety of morphologies have been grown in a facile fashion from readily accessible molecular precursors. Simple synthetic modification of the secondary substituents on the diaryl substituents of the porphyrin rings led to widely different, but understandable, crystal packing arrangements, as well as differing degrees of hydrophobicity. Under conditions of agitated growth, these molecular properties are expressed as diverse macroscopic nanocrystal morphologies. Together with the unique electronic and catalytic properties of the porphyrin building blocks, the ability to assemble these molecular materials into well-defined nano- and macrostructures may enhance the status of porphyrins as candidates for applications in electronics, photonics, and/or catalysis.

Fig. 2 The PXRD patterns for the two nanoparticle samples of **1** as well as that obtained for a single-crystal sample of **1**. a) Nanoplates grown under stirring at rt. b) Nanoplates grown under brief exposure to microwaves at 45 °C. c) Single crystal grown under non-agitated conditions. d) Simulated PXRD pattern obtained from the X-ray crystal structure of **1**.

This journal is © The Royal Society of Chemistry 2008

J. Mater. Chem., 2008, **18**, 3640–3642 | 3641

Fig. 3 Structural, physical, and morphological data for metalloporphyrins **1**, **2** and **3** (for a color version of this figure with clear depiction of the atomic labels, see Fig. S6 in ESI†). From the left: First column: Stick representations of the X-ray structures of the (porphyrin)Sn building blocks. Second column: Photographs of single crystals of **1**, **2** and **3**, and corresponding SEM images of the nanocrystals prepared under agitation. Third column: Packing-diagram representations of the X-ray structures, illustrating the intermolecular H-bonding pattern between adjacent porphyrin layers in **1**, water-mediated H-bonding pattern between adjacent porphyrin layers in **2**, and the absence of such a pattern for **3**. These differences lead to completely different nanoscale morphologies for **1**, **2**, and **3** under agitated growth conditions. Those that can form H-bonds (**1** and **2**) are more likely to afford well-defined nanocrystals while the porphyrin that does not (**3**) tends to yield amorphous nanoparticles. Fourth column: The relative increase in hydrophobicity of thin films of **1**, **2** and **3**, as shown *via* contact-angle measurements (69° for **1**, 74° for **2**, and 83° for **3**) when drops of colored water are placed on top of glass-supported (porphyrin)Sn(OH)$_2$ films. Insets show the side views of the water drops: the most hydrophobic film of **3** cause water to bead up the most.

Notes and references

‡ Synthesis of porphyrin nanoparticles (see also ESI†). Method A: An ethanol solution of porphyrin (200 µL of a 1 mM solution) was injected into a vial containing stirring deionized water (10 mL) at room temperature. Stirring was maintained for approximately 2 to 20 min whereupon suspensions of nanoparticles were obtained. Method B: An ethanol solution of porphyrin (200 µL of a 1 mM solution) was injected into a vial containing stirring deionized water (5 mL) at room temperature. Suspensions of nanoparticles were obtained after 1 to 2 min of microwave irradiation at 45 °C. Isolation of all porphyrin nanoparticles was easily carried out *via* centrifugation and decantation of the mother liquor.

1 (*a*) C. M. Drain, I. Goldberg, I. Sylvain and A. Falber, *Top. Curr. Chem.*, 2005, **245**, 55–88; (*b*) A. Tsuda and A. Osuka, *Science*, 2001, **293**, 79–82; (*c*) K. M. Kadish, K. M. Smith and R. Guilard, *The Porphyrin Handbook, Vol. 6: Applications: Past, Present and Future*, Academic, New York, 2000.

2 (*a*) L.-L. Li, C.-J. Yang, W.-H. Chen and K.-J. Lin, *Angew. Chem., Int. Ed.*, 2003, **42**, 1505–1508; (*b*) T. S. Balaban, R. Goddard, M. Linke-Schaetzel and J.-M. Lehn, *J. Am. Chem. Soc.*, 2003, **125**, 4233–4239; (*c*) T. van der Boom, R. T. Hayes, Y. Zhao, P. J. Bushard, E. A. Weiss and M. R. Wasielewski, *J. Am. Chem. Soc.*, 2002, **124**, 9582–9590.

3 (*a*) S. J. Lee, K. L. Mulfort, X. Zuo, A. J. Goshe, P. J. Wesson, S. T. Nguyen, J. T. Hupp and D. M. Tiede, *J. Am. Chem. Soc.*, 2008, **130**, 836–838; (*b*) F. Hajjaj, Z. S. Yoon, M.-C. Yoon, J. Park, A. Satake, D. Kim and Y. Kobuke, *J. Am. Chem. Soc.*, 2006, **128**, 4612–4623; (*c*) S. J. Lee, K. L. Mulfort, J. L. O'Donnell, X. Zuo, A. J. Goshe, P. J. Wesson, S. T. Nguyen, J. T. Hupp and D. M. Tiede, *Chem. Commun.*, 2006, 4581–4583; (*d*) I.-W. Hwang, T. Kamada, T. K. Ahn, D. M. Ko, T. Nakamura, A. Tsuda, A. Osuka and D. Kim, *J. Am. Chem. Soc.*, 2004, **126**, 16187–16198; (*e*) T. N. Milic, N. Chi, D. G. Yablon, G. W. Flynn, J. D. Batteas and C. M. Drain, *Angew. Chem., Int. Ed.*, 2002, **42**, 2117–2119; (*f*) C. M. Drain, F. Nifiatis, A. Vasenko and J. D. Batteas, *Angew. Chem., Int. Ed.*, 1998, **37**, 2344–2347.

4 For recent reports see (*a*) S. J. Lee, C. D. Malliakas, M. G. Kanatzidis, J. T. Hupp and S. T. Nguyen, *Adv. Mater.*, 2008, DOI: 10.1002/adma.200800003; (*b*) T. Hasobe, H. Oki, A. S. D. Sandanayaka and H. Murata, *Chem. Commun.*, 2008, 724–726; (*c*) Z. Wang, Z. Li, C. J. Medforth and J. A. Shelnutt, *J. Am. Chem. Soc.*, 2007, **129**, 2440–2441; (*d*) B. Liu, D.-J. Qian, M. Chen, T. Wakayama, C. Nakamura and J. Miyake, *Chem. Commun.*, 2006, 3175–3177; (*e*) Z. Wang, K. J. Ho, C. J. Medforth and J. A. Shelnutt, *Adv. Mater.*, 2006, **18**, 2557–2560; (*f*) J.-S. Hu, Y.-G. Guo, H.-P. Liang, L.-J. Wan and L. Jiang, *J. Am. Chem. Soc.*, 2005, **127**, 17090–17095; (*g*) Z. Wang, C. J. Medforth and J. A. Shelnutt, *J. Am. Chem. Soc.*, 2004, **126**, 15954–15955; (*h*) Z. Wang, C. J. Medforth and J. A. Shelnutt, *J. Am. Chem. Soc.*, 2004, **126**, 16720–16721; (*i*) A. D. Schwab, D. E. Smith, B. Bond-Watts, D. E. Johnston, J. Hone, A. T. Johnson, J. C. de Paula and W. F. Smith, *Nano Lett.*, 2004, **4**, 1261–1265.

5 B. J. Littler, M. A. Miller, C.-H. Hung, R. W. Wagner, D. F. O'Shea, P. D. Boyle and J. S. Lindsey, *J. Org. Chem.*, 1999, **64**, 1391–1396.

6 G. S. Wilson and H. L. Anderson, *Chem. Commun.*, 1999, 1539–1540.

7 H.-J. Kim, H. J. Jo, J. Kim, S.-Y. Kim, D. Kim and K. Kim, *CrystEngComm*, 2005, **7**, 417–418.

8 Thin films of (porphyrin)Sn were prepared by depositing a few drops of their CH$_2$Cl$_2$ solutions on glass and slowly evaporating the solvent.

9 (*a*) K. Sendt, L. A. Johnston, W. A. Hough, M. J. Crossley, N. S. Hush and J. R. Reimers, *J. Am. Chem. Soc.*, 2002, **124**, 9299–9309; (*b*) C. A. Hunter, J. K. M. Sanders and A. J. Stone, *Chem. Phys.*, 1989, **133**, 395–404. For a general explanation of the photophysical behavior of macroscopic porphyrin materials, described in terms of J- and H-aggregates, please see: K. M. Kadish, K. M. Smith and R. Guilard, *The Porphyrin Handbook, Vol. 18: Multiporphyrins, Multiphthalocyanines, and Arrays*, Academic, New York, 2000.